Contents

List of Figures

Chapter 15

Bifurcations

15.1 Types of Bifurcations

15.1.1 Saddle-node bifurcation

We remarked above how $f'(u)$ is in general nonzero when $f(u)$ itself vanishes, since two equations in a single unknown is an overdetermined set. However, consider the function $F(x,\alpha)$, where α is a control parameter. If we demand $F(x,\alpha) = 0$ and $\partial_x F(x,\alpha) = 0$, we have two equations in two unknowns, and in general there will be a zero-dimensional solution set consisting of points $(x_{\rm c},\alpha_{\rm c})$. The situation is depicted in Fig. 15.1.

Let's expand $F(x,\alpha)$ in the vicinity of such a point $(x_{\rm c},\alpha_{\rm c})$:

$$\begin{aligned} F(x,\alpha) &= F(x_{\rm c},\alpha_{\rm c}) + \left.\frac{\partial F}{\partial x}\right|_{(x_{\rm c},\alpha_{\rm c})} (x-x_{\rm c}) + \left.\frac{\partial F}{\partial \alpha}\right|_{(x_{\rm c},\alpha_{\rm c})} (\alpha-\alpha_{\rm c}) + \frac{1}{2}\left.\frac{\partial^2 F}{\partial x^2}\right|_{(x_{\rm c},\alpha_{\rm c})} (x-x_{\rm c})^2 \\ &\qquad + \left.\frac{\partial^2 F}{\partial x\,\partial \alpha}\right|_{(x_{\rm c},\alpha_{\rm c})} (x-x_{\rm c})\,(\alpha-\alpha_{\rm c}) + \frac{1}{2}\left.\frac{\partial^2 F}{\partial \alpha^2}\right|_{(x_{\rm c},\alpha_{\rm c})} (\alpha-\alpha_{\rm c})^2 + \dots \qquad (15.1) \\ &= A\,(\alpha-\alpha_{\rm c}) + B\,(x-x_{\rm c})^2 + \dots\ , \qquad (15.2) \end{aligned}$$

where we keep terms of lowest order in the deviations δx and $\delta\alpha$. Note that we can separately change the signs of A and B by redefining $\alpha \to -\alpha$ and/or $x \to -x$, so without loss of generality we may assume both A and B are positive. If we now rescale $u \equiv \sqrt{B/A}\,(x-x_{\rm c})$, $r \equiv \alpha - \alpha_{\rm c}$, and $\tau = \sqrt{AB}\,t$, we have, neglecting the higher order terms, we obtain the 'normal form' of the saddle-node bifurcation,

$$\frac{du}{d\tau} = r + u^2\ . \qquad (15.3)$$

The evolution of the flow is depicted in Fig. 15.2. For $r < 0$ there are two fixed points – one stable ($u^* = -\sqrt{-r}$) and one unstable ($u = +\sqrt{-r}$). At $r = 0$ these two nodes coalesce and annihilate each other. (The point $u^* = 0$ is half-stable precisely at $r = 0$.) For $r > 0$ there are no longer any fixed points

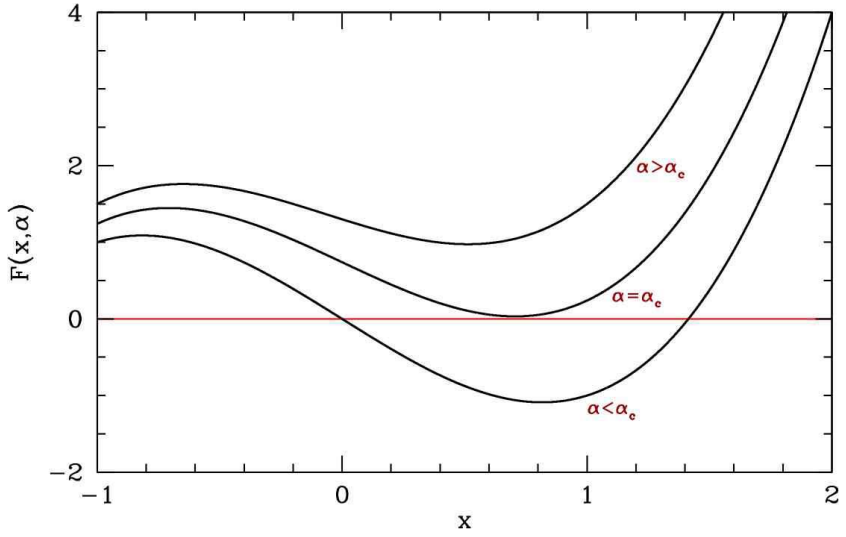

Figure 15.1: Evolution of $F(x,\alpha)$ as a function of the control parameter α.

in the vicinity of $u = 0$. In the left panel of Fig. 15.3 we show the flow in the extended (r, u) plane. The unstable and stable nodes annihilate at $r = 0$.

15.1.2 Transcritical bifurcation

Another situation which arises frequently is the *transcritical bifurcation*. Consider the equation $\dot{x} = f(x)$ in the vicinity of a fixed point x^*.

$$\frac{dx}{dt} = f'(x^*)\,(x - x^*) + \tfrac{1}{2}\,f''(x^*)(x - x^*)^2 + \ldots \ . \tag{15.4}$$

We rescale $u \equiv \beta\,(x - x^*)$ with $\beta = -\frac{1}{2}\,f''(x^*)$ and define $r \equiv f'(x^*)$ as the control parameter, to obtain, to order u^2,

$$\frac{du}{dt} = ru - u^2 \ . \tag{15.5}$$

Note that the sign of the u^2 term can be reversed relative to the others by sending $u \to -u$.

Consider a crude model of a laser threshold. Let n be the number of photons in the laser cavity, and N the number of excited atoms in the cavity. The dynamics of the laser are approximated by the equations

$$\begin{aligned} \dot{n} &= GNn - kn \\ N &= N_0 - \alpha n \ . \end{aligned} \tag{15.6}$$

Here G is the gain coefficient and k the photon decay rate. N_0 is the pump strength, and α is a numerical factor. The first equation tells us that the number of photons in the cavity grows with a rate $GN - k$; gain is proportional to the number of excited atoms, and the loss rate is a constant cavity-dependent quantity (typically through the ends, which are semi-transparent). The second equation says that the number of

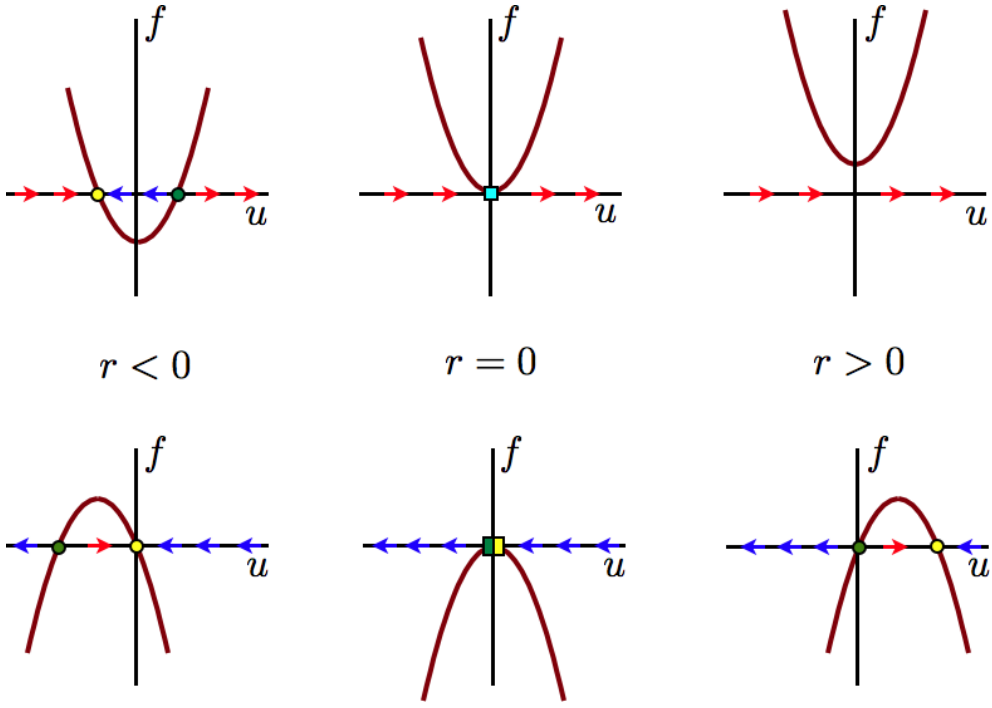

Figure 15.2: Flow diagrams for the saddle-node bifurcation $\dot{u} = r + u^2$ (top) and the transcritical bifurcation $\dot{u} = ru - u^2$ (bottom).

excited atoms is equal to the pump strength minus a term proportional to the number of photons (since the presence of a photon means an excited atom has decayed). Putting them together,

$$\dot{n} = (GN_0 - k)\, n - \alpha G n^2 \,, \tag{15.7}$$

which exhibits a transcritical bifurcation at pump strength $N_0 = k/G$. For $N_0 < k/G$ the system acts as a lamp; for $N_0 > k/G$ the system acts as a laser.

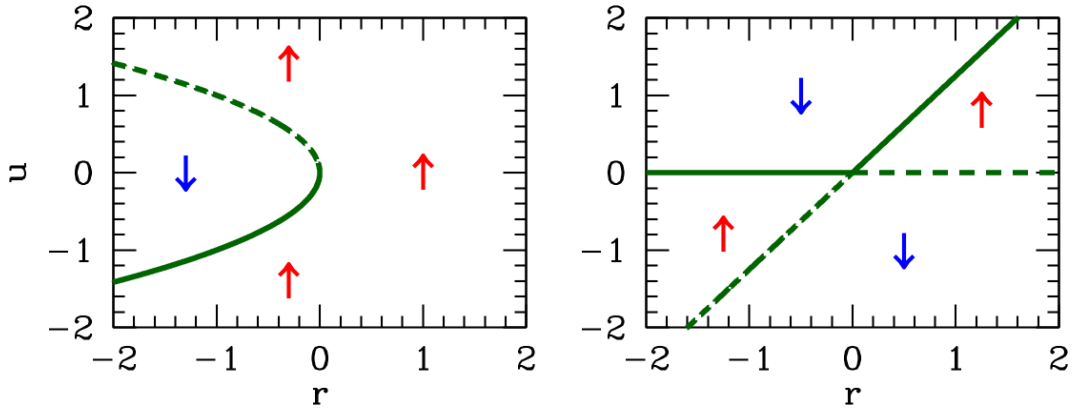

Figure 15.3: Extended phase space (r, u) flow diagrams for the saddle-node bifurcation $\dot{u} = r + u^2$ (left) and the transcritical bifurcation $\dot{u} = ru - u^2$ (right).

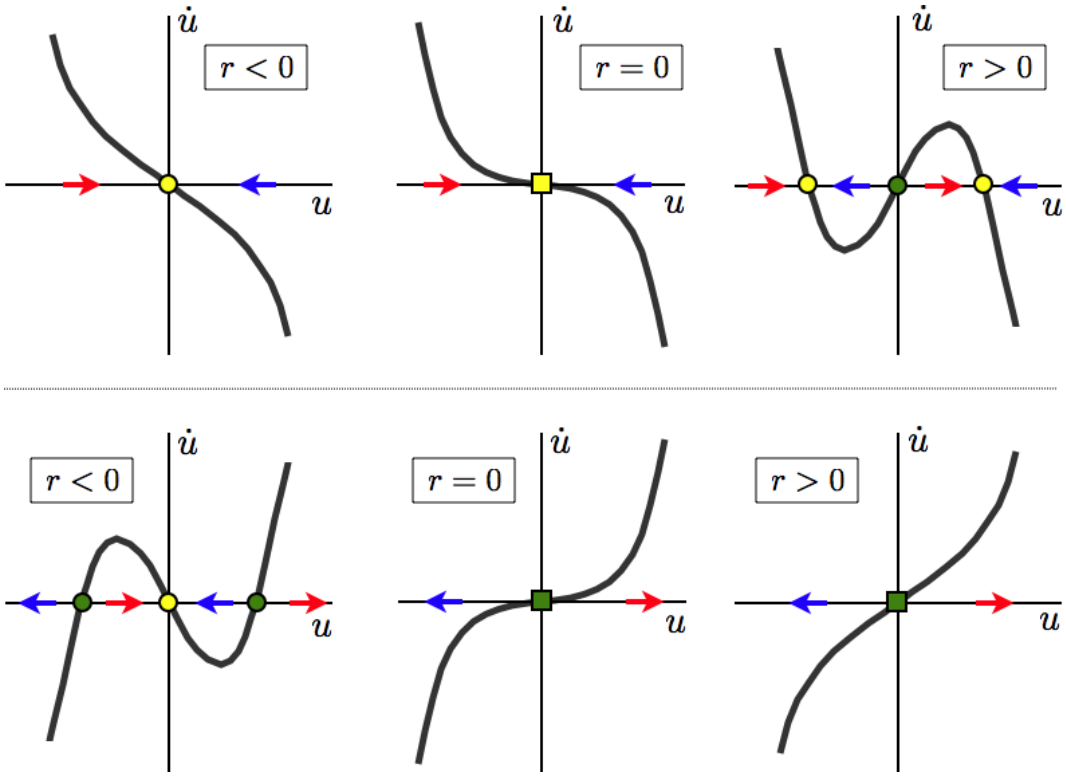

Figure 15.4: Top: supercritical pitchfork bifurcation $\dot{u} = ru - u^3$. Bottom: subcritical pitchfork bifurcation $\dot{u} = ru + u^3$.

What happens in the transcritical bifurcation is an exchange of stability of the fixed points at $u^* = 0$ and $u^* = r$ as r passes through zero. This is depicted graphically in the bottom panel of Fig. 15.2.

15.1.3 Pitchfork bifurcation

The pitchfork bifurcation is commonly encountered in systems in which there is an overall parity symmetry ($u \to -u$). There are two classes of pitchfork: supercritical and subcritical. The normal form of the supercritical bifurcation is

$$\dot{u} = ru - u^3 \,, \tag{15.8}$$

which has fixed points at $u^* = 0$ and $u^* = \pm\sqrt{r}$. Thus, the situation is as depicted in fig. 15.4 (top panel). For $r < 0$ there is a single stable fixed point at $u^* = 0$. For $r > 0$, $u^* = 0$ is unstable, and flanked by two stable fixed points at $u^* = \pm\sqrt{r}$.

If we send $u \to -u$, $r \to -r$, and $t \to -t$, we obtain the *subcritical pitchfork*, depicted in the bottom panel of fig. 15.4. The normal form of the subcritical pitchfork bifurcation is

$$\dot{u} = ru + u^3 \,. \tag{15.9}$$

The fixed point structure in both supercritical and subcritical cases is shown in Fig. 15.5.

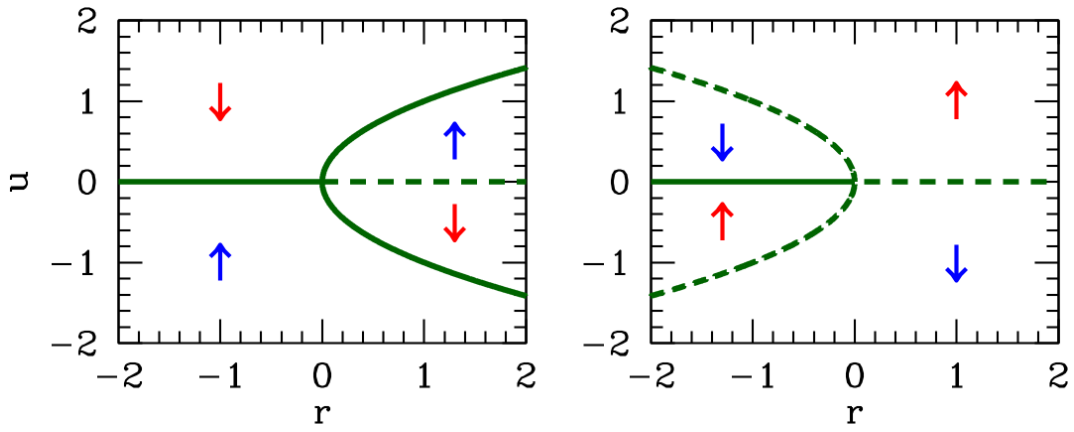

Figure 15.5: Extended phase space (r, u) flow diagrams for the supercritical pitchfork bifurcation $\dot{u} = ru - u^3$ (left), and subcritical pitchfork bifurcation $\dot{u} = ru + u^3$ (right).

15.1.4 Imperfect bifurcation

The imperfect bifurcation occurs when a symmetry-breaking term is added to the pitchfork. The normal form contains two control parameters:

$$\dot{u} = h + ru - u^3 \ . \tag{15.10}$$

Here, the constant h breaks the parity symmetry if $u \to -u$.

This equation arises from a crude model of magnetization dynamics. Let M be the magnetization of a sample, and $F(M)$ the free energy. Assuming M is small, we can expand $F(M)$ as

$$F(M) = -HM + \tfrac{1}{2}aM^2 + \tfrac{1}{4}bM^4 + \ldots \ , \tag{15.11}$$

where H is the external magnetic field, and a and b are temperature-dependent constants. This is called the *Landau expansion* of the free energy. We assume $b > 0$ in order that the minimum of $F(M)$ not lie at infinity. The dynamics of $M(t)$ are modeled by

$$\frac{dM}{dt} = -\Gamma \frac{\partial F}{\partial M} \ , \tag{15.12}$$

with $\Gamma > 0$. Thus, the magnetization evolves toward a local minimum in the free energy. Note that the free energy is a decreasing function of time:

$$\frac{dF}{dt} = \frac{\partial F}{\partial M}\frac{dM}{dt} = -\Gamma\left(\frac{\partial F}{\partial M}\right)^2 \ . \tag{15.13}$$

By rescaling $M \equiv uM_0$ with $M_0 = (b\,\Gamma)^{-1/2}$ and defining $r \equiv -a\Gamma$ and $h \equiv (\Gamma^3\, b)^{1/2}\, H$, we obtain the normal form

$$\begin{aligned} \dot{u} = h + ru - u^3 &= -\frac{\partial f}{\partial u} \\ f(u) &= -\tfrac{1}{2}ru^2 + \tfrac{1}{4}u^4 - hu \ . \end{aligned} \tag{15.14}$$

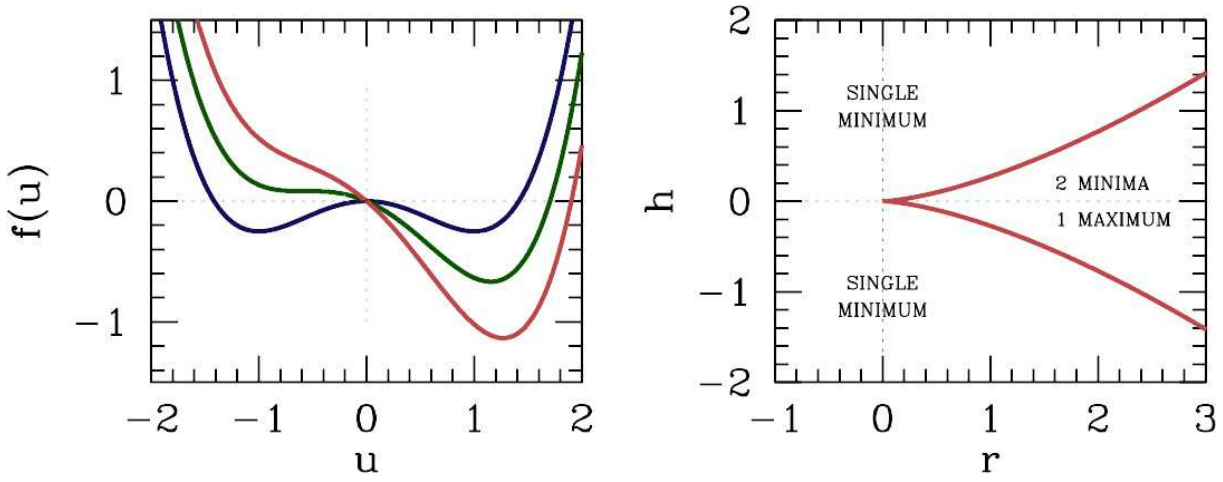

Figure 15.6: Left: scaled free energy $f(u) = -\frac{1}{2}ru^2 + \frac{1}{4}u^4 - hu$, with $h = 0$ (blue), $h = h_{\rm c}$ (green), and $h = 2h_{\rm c}$ (red), where $h_{\rm c} = \frac{2}{3\sqrt{3}}\, r^{3/2}$. Right: phase diagram for the imperfect bifurcation $\dot{u} = -f'(u) = h + ru - u^3$ in the (r, h) plane.

Here, $f(u)$ is a scaled version of the free energy.

Fixed points satisfy the equation

$$u^3 - ru - h = 0\,, \tag{15.15}$$

and correspond to extrema in $f(u)$. By the fundamental theorem of algebra, this cubic polynomial may be uniquely factorized over the complex plane. Since the coefficients are real, the complex conjugate $\bar{u}$ satisfies the same equation as u, hence there are two possibilities for the roots: either (i) all three roots are real, or (ii) one root is real and the other two are a complex conjugate pair. Clearly for $r < 0$ we are in situation (ii) since $u^3 - ru$ is then monotonically increasing for $u \in \mathbb{R}$, and therefore takes the value h precisely once for u real. For $r > 0$, there is a region $h \in \big[-h_{\rm c}(r), h_{\rm c}(r)\big]$ over which there are three real roots. To find $h_{\rm c}(r)$, we demand $f''(u) = 0$ as well as $f'(u) = 0$, which says that two roots have merged, forming an inflection point. One easily finds $h_{\rm c}(r) = \frac{2}{3\sqrt{3}}\, r^{3/2}$.

Examples of the function $f(u)$ for $r > 0$ are shown in the left panel of Fig. 15.6 for three different values of h. For $|h| < h_{\rm c}(r)$ there are three extrema satisfying $f'(u^*) = 0$: $u_1^* < u_2^* < 0 < u_3^*$, assuming (without loss of generality) that $h > 0$. Clearly u_1^* is a local minimum, u_2^* a local maximum, and u_3^* the global minimum of the function $f(u)$. The 'phase diagram' for this system, plotted in the (r, h) control parameter space, is shown in the right panel of Fig. 15.6.

In Fig. 15.7 we plot the fixed points $u^*(r)$ for fixed h. A saddle-node bifurcation occurs at $r = r_{\rm c}(h) = \frac{3}{2^{2/3}}\,|h|^{2/3}$. For $h = 0$ this reduces to the supercritical pitchfork; for finite h the pitchfork is deformed and even changed topologically. Finally, in Fig. 15.7 we show the behavior of $u^*(h)$ for fixed r. When $r < 0$ the curve retraces itself as h is ramped up and down, but for $r > 0$ the system exhibits the phenomenon of *hysteresis*, *i.e.* there is an irreversible aspect to the behavior. Fig, 15.7 shows a *hysteresis loop* when $r > 0$.

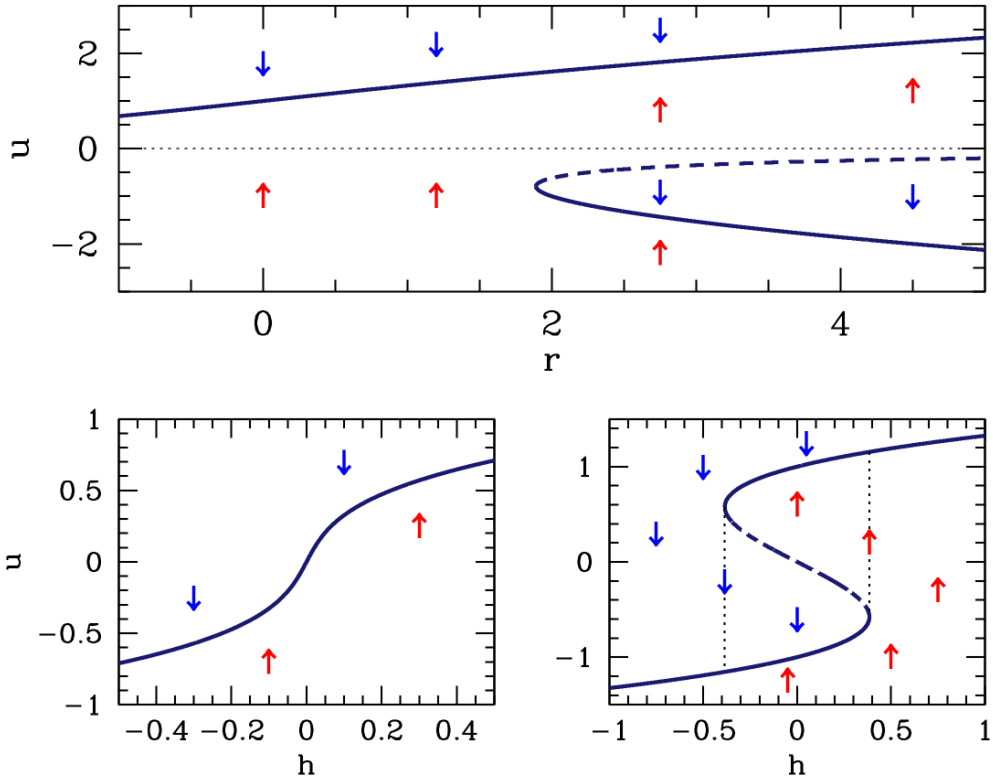

Figure 15.7: Top: extended phase space (r, u) flow diagram for the imperfect pitchfork bifurcation $\dot{u} = h + ru - u^3$ for $h = 1$. This is in a sense a deformed supercritical pitchfork. Bottom: extended phase space (h, u) flow diagram for the imperfect pitchfork bifurcation $r = -0.2$ (left panel) and $r = 1$ (right panel). For $r < 0$ the behavior is completely reversible. For $r > 0$, a regime of irreversibility sets in between $-h_c$ and $+h_c$, where $h_c = 2(r/3)^{3/2}$. The system then exhibits the phenomenon of hysteresis. The dotted vertical lines show the boundaries of the hysteresis loop.

15.2 Examples

15.2.1 Population dynamics

Consider the dynamics of a harvested population,

$$\dot{N} = rN\left(1 - \frac{N}{K}\right) - H(N)\,, \tag{15.16}$$

where $r, K > 0$, and where $H(N)$ is the *harvesting rate*.

(a) Suppose $H(N) = H_0$ is a constant. Sketch the phase flow, and identify and classify all fixed points.

Solution : We examing $\dot{N} = f(N)$ with

$$f(N) = rN - \frac{r}{K}\,N^2 - H_0\,. \tag{15.17}$$

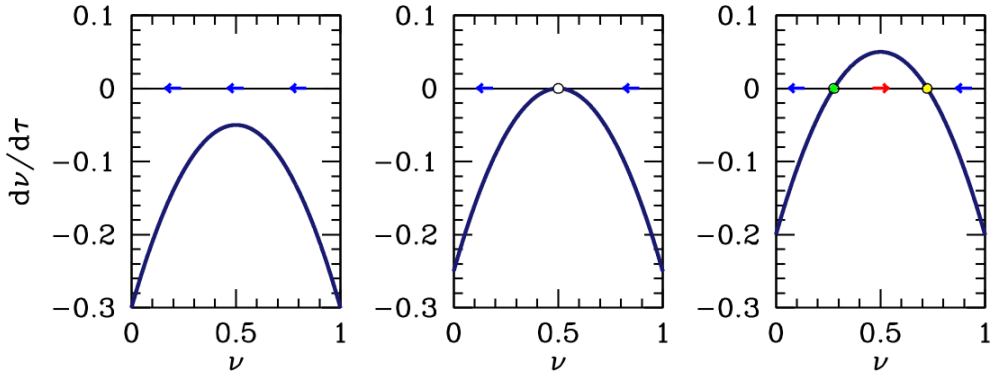

Figure 15.8: Phase flow for the constantly harvested population, $\dot\nu = \nu(1-\nu) - h$, for $h = 0.30$ (left), $h = 0.25$ (center), and $h = 0.20$ (right). The critical harvesting rate is $h_{\rm c} = \frac{1}{4}$.

Setting $f'(N) = 0$ yields $N = \frac{1}{2}K$. $f(N)$ is a downward-opening parabola whose maximum value is $f\big(\frac{1}{2}K\big) = \frac{1}{4}rK - H_0$. Thus, if $H_0 > \frac{1}{4}rK$, the harvesting rate is too large and the population always shrinks. A saddle-node bifurcation occurs at this value of H_0, and for larger harvesting rates, there are fixed points at

$$N_\pm = \tfrac{1}{2}K \pm \tfrac{1}{2}K\sqrt{1 - \frac{4H_0}{rK}}\ , \tag{15.18}$$

with N_- unstable and N_+ stable. By rescaling the population $\nu = N/K$, time $\tau = rt$ and harvesting rate $h = H_0/rK$, we arrive at the equation

$$\dot\nu = \nu(1-\nu) - h\ . \tag{15.19}$$

The critical harvesting rate is then $h_{\rm c} = \frac{1}{4}$. See fig. 15.8.

(b) One defect of the constant harvesting rate model is that $N = 0$ is not a fixed point. To remedy this, consider the following model for $H(N)$[1]:

$$H(N) = \frac{B\,N^2}{N^2 + A^2}\ , \tag{15.20}$$

where A and B are (positive) constants. Show that one can rescale (N, t) to (n, τ), such that

$$\frac{dn}{d\tau} = \gamma\, n\left(1 - \frac{n}{c}\right) - \frac{n^2}{n^2+1}\ , \tag{15.21}$$

where γ and c are positive constants. Provide expressions for n, τ, γ, and c.

Solution : Examining the denominator of $H(N)$, we must take $N = An$. Dividing both sides of $\dot N = f(N)$ by B, we obtain

$$\frac{A}{B}\frac{dN}{dt} = \frac{rA}{B}\,n\Big(1 - \frac{A}{K}\,n\Big) - \frac{n^2}{n^2+1}\ ,$$

from which we glean $\tau = Bt/A$, $\gamma = rA/B$, and $c = K/A$.

[1]This is a model for the dynamics of the spruce budworm population, taken from ch. 1 of J. D. Murray, *Mathematical Biology* (2nd edition, Springer, 1993).

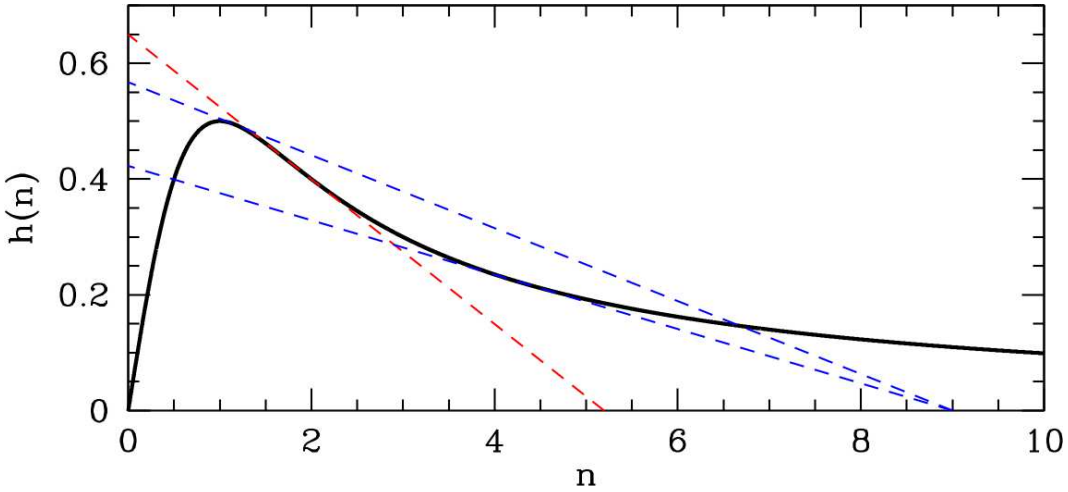

Figure 15.9: Plot of $h(n) = n/(n^2+1)$ (thick black curve). Straight lines show the function $y(n) = \gamma\left(1-\frac{n}{c}\right)$ for different values of c and γ. The red line is tangent to the inflection point of $h(n)$ and determines the minimum value $c^* = 3\sqrt{3}$ for a bifurcation. The blue lines show the construction for determining the location of the two bifurcations for $c > c^*$ (in this case, $c = 9$). See the analysis in the text.

(c) Show that for c sufficiently small that there is a unique asymptotic ($\tau \to \infty$) value for the (scaled) population n, for any given value of γ. Thus, there are no bifurcations as a function of the control parameter γ for c fixed and $c < c^*$.

(d) Show that for $c > c^*$, there are two bifurcations as a function of γ, and that for $\gamma_1^* < \gamma < \gamma_2^*$ the asymptotic solution is bistable, *i.e.* there are two stable values for $n(\tau \to \infty)$. Sketch the solution set 'phase diagram' in the (c, γ) plane. *Hint: Sketch the functions* $\gamma(1-n/c)$ *and* $n/(n^2+1)$. *The* $n \neq 0$ *fixed points are given by the intersections of these two curves. Determine the boundary of the bistable region in the* (c, γ) *plane parametrically in terms of* n. Find c^* and $\gamma_1^*(c) = \gamma_2^*(c)$.

Solution (c) *and* (d) : We examine

$$\frac{dn}{d\tau} = g(n) = \left\{\gamma\Big(1 - \frac{n}{c}\Big) - \frac{n}{n^2+1}\right\} n \ . \tag{15.22}$$

There is an unstable fixed point at $n = 0$, where $g'(0) = \gamma > 0$. The other fixed points occur when the term in the curvy brackets vanishes. In fig. 15.9 we plot the function $h(n) \equiv n/(n^2+1)$ *versus* n. We seek the intersection of this function with a two-parameter family of straight lines, given by $y(n) = \gamma\,(1-n/c)$. The n-intercept is c and the y-intercept is γ. Provided $c > c^*$ is large enough, there are two bifurcations as a function of γ, which we call $\gamma_\pm(c)$. These are shown as the dashed blue lines in figure 15.9 for $c = 9$.

Both bifurcations are of the saddle-node type. We determine the curves $\gamma_\pm(c)$ by requiring that $h(n)$ is tangent to $y(n)$, which gives two equations:

$$\begin{aligned} h(n) &= \frac{n}{n^2+1} = \gamma\Big(1 - \frac{n}{c}\Big) = y(n) \\ h'(n) &= \frac{1-n^2}{(n^2+1)^2} = -\frac{\gamma}{c} = y'(n) \ . \end{aligned} \tag{15.23}$$

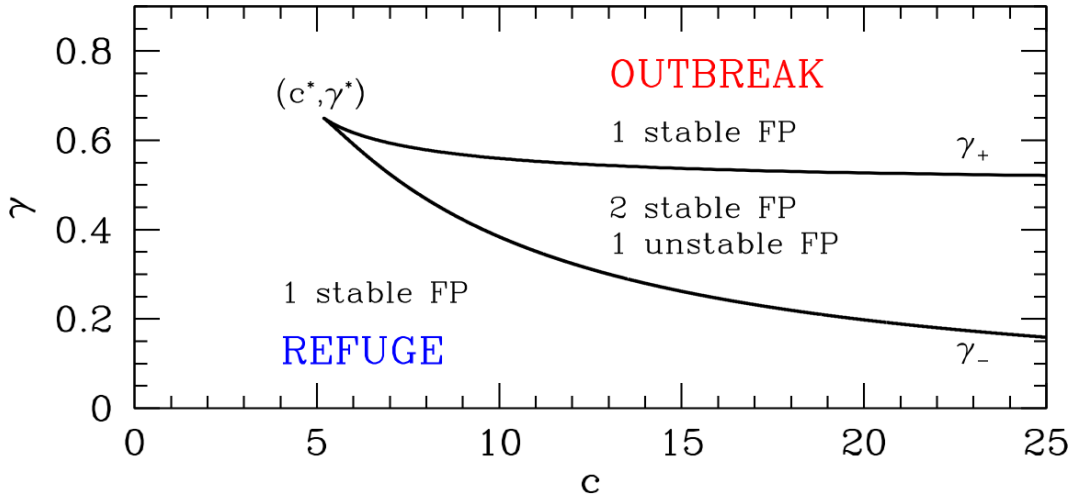

Figure 15.10: Phase diagram for the equation $\dot{n} = \gamma(1 - n/c)\, n - n^2/(n^2+1)$, labeling $n \neq 0$ fixed points. (The point $n = 0$ is always unstable.)

Together, these give $\gamma(c)$ parametrically, *i.e.* as $\gamma(n)$ and $c(n)$:

$$\gamma(n) = \frac{2n^3}{(n^2+1)^2} \qquad , \qquad c(n) = \frac{2n^3}{(n^2-1)} \; . \tag{15.24}$$

Since $h(n)$ is maximized for $n = 1$, where $h(1) = \frac{1}{2}$, there is no bifurcation occurring at values $n < 1$. If we plot $\gamma(n)$ *versus* $c(n)$ over the allowed range of n, we obtain the phase diagram in fig. 15.10. The cusp occurs at (c^*, γ^*), and is determined by the requirement that the two bifurcations coincide. This supplies a third condition, namely that $h''(n) = 0$, where

$$h''(n) = \frac{2n\,(n^2-3)}{(n^2+1)^3} \; . \tag{15.25}$$

Thus $n = \sqrt{3}$, whence $c^* = 3\sqrt{3}$ and $\gamma^* = \frac{3\sqrt{3}}{8}$. For $c < c^*$, there are no bifurcations at any value of γ.

15.2.2 The Bletch

Problem: The bletch is a disgusting animal native to the Forest of Jkroo on the planet Barney. The bletch population obeys the equation

$$\frac{dN}{dt} = aN^2 - bN^3 \; , \tag{15.26}$$

where N is the number of bletches, and a and b are constants. (Bletches reproduce asexually, but only when another bletch is watching. However, when there are three bletches around, they beat the `@!!*$&*` out of each other.)

(a) Sketch the phase flow for N. (Strange as the bletch is, you can still rule out $N < 0$.) Identify and classify all fixed points.

Figure 15.11: Phase flow for the scaled bletch population, $\dot{n} = n^2 - n^3$.

(b) The bletch population is now *harvested* (they make nice shoes). To model this, we add an extra term to the dynamics:

$$\frac{dN}{dt} = -hN + aN^2 - bN^3 \,, \tag{15.27}$$

where h is the harvesting rate. Show that the phase flow now depends crucially on h, in that there are two qualitatively different flows, depending on whether $h < h_c(a,b)$ or $h > h_c(a,b)$. Find the critical harvesting rate $h_c(a,b)$ and sketch the phase flows for the two different regimes.

(c) In equilibrium, the rate at which bletches are harvested is $R = hN^*$, where N^* is the equilibrium bletch population. Suppose we start with $h = 0$, in which case N^* is given by the value of N at the stable fixed point you found in part (a). Now let h be increased very slowly from zero. As h is increased, the equilibrium population changes. Sketch R *versus* h. What value of h achieves the biggest bletch harvest? What is the corresponding value of $R_{\rm max}$?

Solution:

(a) Setting the RHS of eqn. 15.26 to zero suggests the rescaling

$$N = \frac{a}{b}\,n \qquad , \qquad t = \frac{b}{a^2}\,\tau \,. \tag{15.28}$$

This results in

$$\frac{dn}{d\tau} = n^2 - n^3 \,. \tag{15.29}$$

The point $n = 0$ is a (nonlinearly) repulsive fixed point, and $n = 1$, corresponding to $N = a/b$, is attractive. The flow is shown in fig. 15.11.

By the way, the dynamics can be integrated, using the method of partial fractions, to yield

$$\frac{1}{n_0} - \frac{1}{n} + \ln\left(\frac{n}{n_0}\cdot\frac{1-n_0}{1-n}\right) = \tau \,. \tag{15.30}$$

(b) Upon rescaling, the harvested bletch dynamics obeys the equation

$$\frac{dn}{d\tau} = -\nu n + n^2 - n^3 \,, \tag{15.31}$$

where $\nu = bh/a^2$ is the dimensionless harvesting rate. Setting the RHS to zero yields $n(n^2 - n + \nu) = 0$, with solutions $n^* = 0$ and

$$n^*_\pm = \tfrac{1}{2} \pm \sqrt{\tfrac{1}{4} - \nu} \,. \tag{15.32}$$

At $\nu = \frac{1}{4}$ there is a saddle-node bifurcation, and for $\nu > \frac{1}{4}$ the only fixed point (for real n) is at $n^* = 0$ (stable) – the bletch population is then *overharvested*. For $\nu > \frac{1}{4}$, there are three solutions: a

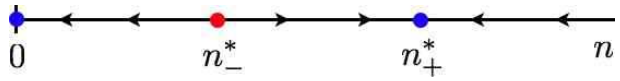

Figure 15.12: Phase flow for the harvested bletch population, $\dot{n} = -\nu n + n^2 - n^3$.

stable fixed point at $n^* = 0$, an unstable fixed point at $n^* = \frac{1}{2} - \sqrt{\frac{1}{4} - \nu}$, and a stable fixed point at $n^* = \frac{1}{2} + \sqrt{\frac{1}{4} - \nu}$. The critical harvesting rate is $\nu_{\rm c} = \frac{1}{4}$, which means $h_{\rm c} = a^2/4b$.

(c) The scaled bletch harvest is given by $r = \nu\, n^*_+(\nu)$. Note $R = h\, N^*_+ = \frac{a^3}{b^2}\, r$. The optimal harvest occurs when $\nu\, n^*$ is a maximum, which means we set

$$\frac{d}{d\nu}\left\{\tfrac{1}{2}\nu + \nu\sqrt{\tfrac{1}{4} - \nu}\right\} = 0 \quad \Longrightarrow \quad \nu_{\rm opt} = \tfrac{2}{9}\,. \tag{15.33}$$

Thus, $n^*_+(\nu_{\rm opt}) = \frac{2}{3}$ and $r_{\rm opt} = \frac{4}{27}$, meaning $R = 4a^3/27\,b^2$. Note that at $\nu = \nu_{\rm c} = \frac{1}{4}$ that $n^*_+(\nu_{\rm c}) = \frac{1}{2}$, hence $r(\nu_{\rm c}) = \frac{1}{8}$, which is smaller than $(\nu_{\rm opt}) = \frac{2}{3}$. The harvest $r(\nu)$ discontinuously drops to zero at $\nu = \nu_{\rm c}$, since for $\nu > \nu_{\rm c}$ the flow is to the only stable fixed point at $n^* = 0$.

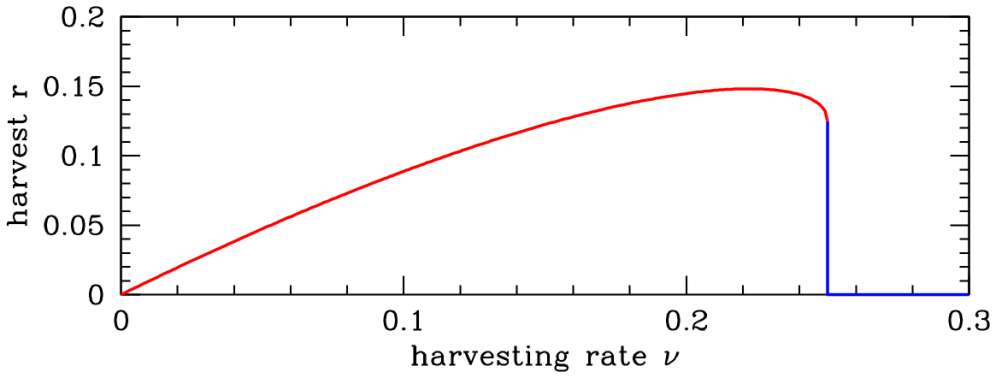

Figure 15.13: Scaled bletch harvest r *versus* scaled harvesting rate ν. Optimal harvesting occurs for $\nu_{\rm opt} = \frac{2}{9}$. The critical harvesting rate is $\nu_{\rm c} = \frac{1}{4}$, at which point the harvest discontinuously drops to zero.

15.3 Appendix : Landau Theory of Phase Transitions

Landau's theory of phase transitions is based on an expansion of the free energy of a thermodynamic system in terms of an *order parameter*, which is nonzero in an ordered phase and zero in a disordered phase. For example, the magnetization M of a ferromagnet in zero external field but at finite temperature typically vanishes for temperatures $T > T_{\rm c}$, where $T_{\rm c}$ is the *critical temperature*, also called the *Curie temperature* in a ferromagnet. A low order expansion in powers of the order parameter is appropriate sufficiently close to $T_{\rm c}$, *i.e.* at temperatures such that the order parameter, if nonzero, is still small.

The simplest example is the quartic free energy,

$$f(m) = f_0 + \tfrac{1}{2}am^2 + \tfrac{1}{4}bm^4\,, \tag{15.34}$$

where m is a dimensionless measure of the magnetization density, and where f_0, a, and b are all functions of the dimensionless temperature θ, which in a ferromagnet is the ratio $\theta = k_{\rm B}T/\mathcal{J}$, where $\mathcal{J} = \sum_j J_{ij}$ is a sum over the couplings. Let us assume $b > 0$, which is necessary if the free energy is to be bounded from below[2]. The equation of state ,

$$\frac{\partial f}{\partial m} = 0 = am + bm^3 \ , \tag{15.35}$$

has three solutions in the complex m plane: (i) $m = 0$, (ii) $m = \sqrt{-a/b}$, and (iii) $m = -\sqrt{-a/b}$. The latter two solutions lie along the (physical) real axis if $a < 0$. We assume that $a(\theta$ is monotonically increasing, and that there exists a unique temperature $\theta_{\rm c}$ where $a(\theta_{\rm c}) = 0$. Minimizing f, we find

$$\begin{aligned} \theta < \theta_{\rm c} \quad &: \quad f = f_0 - \frac{a^2}{4b} \\ \theta > \theta_{\rm c} \quad &: \quad f = f_0 \ . \end{aligned} \tag{15.36}$$

The free energy is continuous at $\theta_{\rm c}$ since $a(\theta_{\rm c}) = 0$. The specific heat, however, is discontinuous across the transition, with

$$c\big(\theta_{\rm c}^+\big) - c\big(\theta_{\rm c}^-\big) = -\theta_{\rm c}\,\frac{\partial^2}{\partial\theta^2}\bigg|_{\theta=\theta_{\rm c}}\left(\frac{a^2}{4b}\right) = -\frac{\theta_{\rm c}\left[a'(\theta_{\rm c})\right]^2}{2b(\theta_{\rm c})} \ . \tag{15.37}$$

The presence of a magnetic field h breaks the $\mathbb{Z}_2$ symmetry of $m \to -m$. The free energy becomes

$$f(m) = f_0 + \tfrac{1}{2}am^2 + \tfrac{1}{4}bm^4 - hm \ , \tag{15.38}$$

and the mean field equation is

$$bm^3 + am - h = 0 \ . \tag{15.39}$$

This is a cubic equation for m with real coefficients, and as such it can either have three real solutions or one real solution and two complex solutions related by complex conjugation. Clearly we must have $a < 0$ in order to have three real roots, since $bm^3 + am$ is monotonically increasing otherwise. The boundary between these two classes of solution sets occurs when two roots coincide, which means $f''(m) = 0$ as well as $f'(m) = 0$. Simultaneously solving these two equations, we find

$$h^*(a) = \pm\frac{2}{3^{3/2}}\,\frac{(-a)^{3/2}}{b^{1/2}} \ , \tag{15.40}$$

or, equivalently,

$$a^*(h) = -\frac{3}{2^{2/3}}\,b^{1/3}\,|h|^{2/3}. \tag{15.41}$$

If, for fixed h, we have $a < a^*(h)$, then there will be three real solutions to the mean field equation $f'(m) = 0$, one of which is a global minimum (the one for which $m \cdot h > 0$). For $a > a^*(h)$ there is only a single global minimum, at which m also has the same sign as h. If we solve the mean field equation perturbatively in h/a, we find

$$\begin{aligned} m(a,h) &= \frac{h}{a} - \frac{b\,h^3}{a^4} + \mathcal{O}(h^5) \qquad\qquad (a > 0) \\ &= \frac{h}{2\,|a|} - \frac{3\,b^{1/2}\,h^2}{8\,|a|^{5/2}} + \mathcal{O}(h^3) \qquad (a < 0) \ . \end{aligned} \tag{15.42}$$

[2]It is always the case that f is bounded from below, on physical grounds. Were b negative, we'd have to consider higher order terms in the Landau expansion.

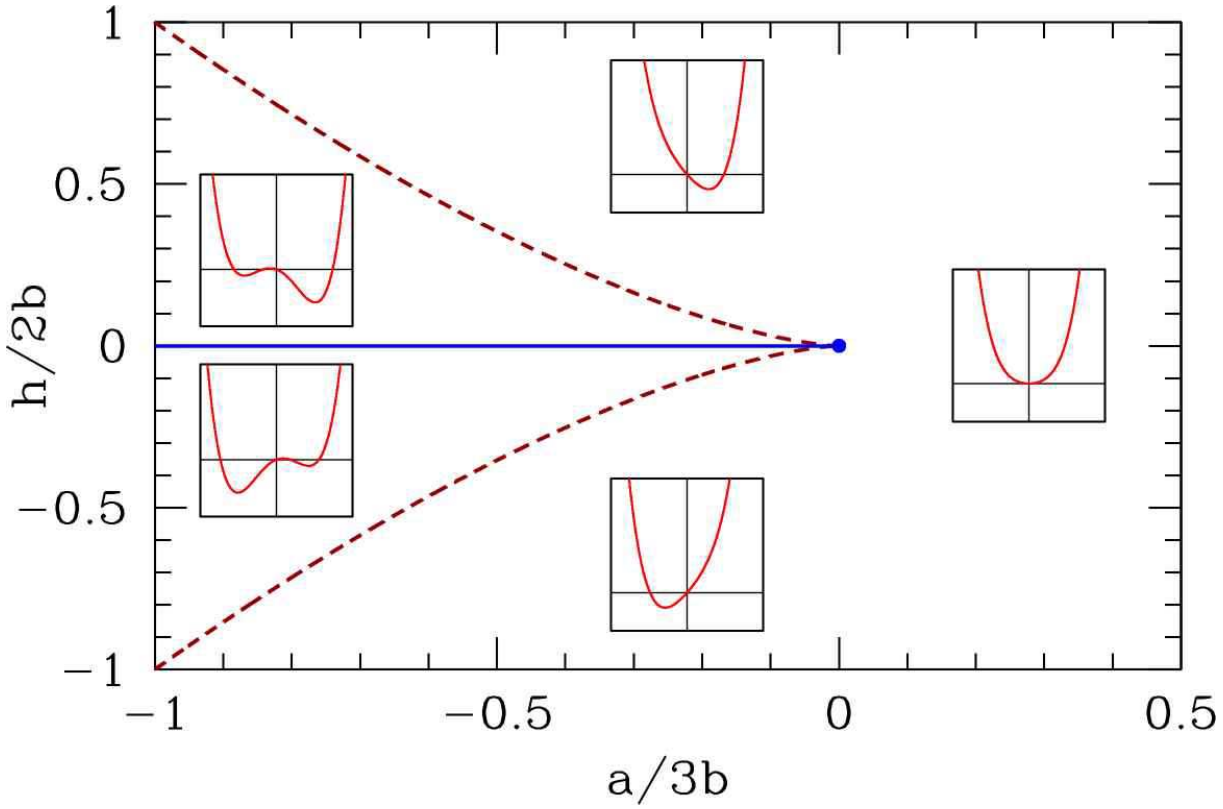

Figure 15.14: Phase diagram for the quartic mean field theory $f = f_0 + \frac{1}{2}am^2 + \frac{1}{4}bm^4 - hm$, with $b > 0$. There is a first order line at $h = 0$ extending from $a = -\infty$ and terminating in a critical point at $a = 0$. For $|h| < h^*(a)$ (dashed red line) there are three solutions to the mean field equation, corresponding to one global minimum, one local minimum, and one local maximum. Insets show behavior of the free energy $f(m)$.

15.3.1 Landau coefficients from mean field theory

A simple variational density matrix for the Ising ferromagnet yields the dimensionless free energy density

$$f(m,h,\theta) = -\tfrac{1}{2}\,m^2 - hm + \theta\left\{\left(\frac{1+m}{2}\right)\ln\left(\frac{1+m}{2}\right) + \left(\frac{1-m}{2}\right)\ln\left(\frac{1-m}{2}\right)\right\}. \tag{15.43}$$

When m is small, it is appropriate to expand $f(m,h,\theta)$, obtaining

$$f(m,h,\theta) = -\theta\,\ln 2 - hm + \tfrac{1}{2}(\theta-1)\,m^2 + \tfrac{\theta}{12}\,m^4 + \tfrac{\theta}{30}\,m^6 + \tfrac{\theta}{56}\,m^8 + \ldots\,. \tag{15.44}$$

Thus, we identify

$$a(\theta) = \theta - 1 \qquad , \qquad b(\theta) = \tfrac{1}{3}\theta\,. \tag{15.45}$$

We see that $a(\theta) = 0$ at a critical temperature $\theta_{\rm c} = 1$.

The free energy of eqn. 15.43 behaves qualitatively just like it does for the simple Landau expansion, where one stops at order m^4. Consider without loss of generality the case $h > 0$. The minimum of the

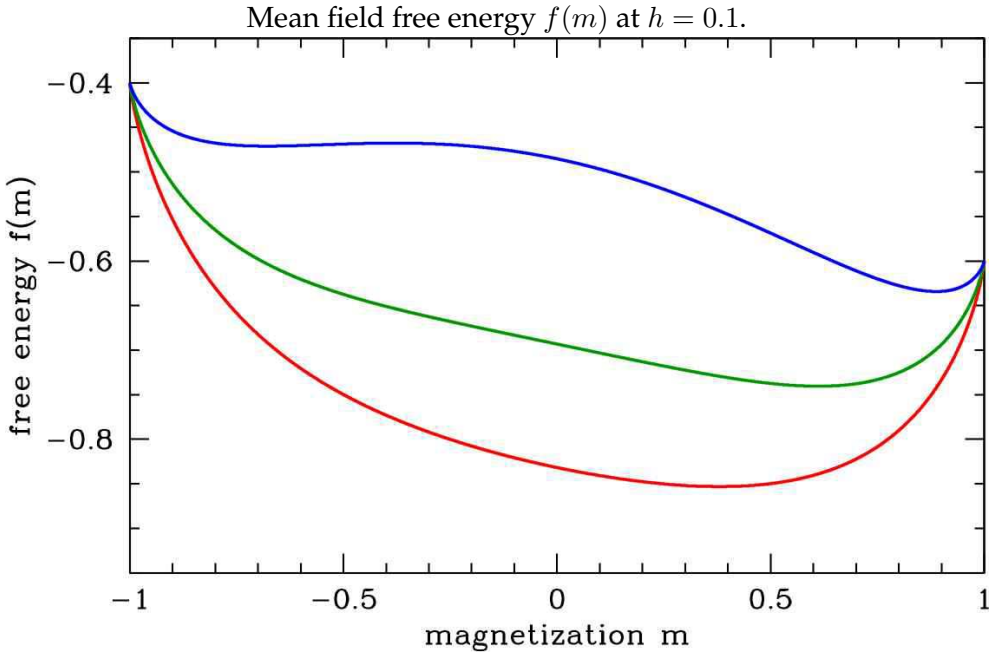

Figure 15.15: Mean field free energy $f(m)$ at $h = 0.1$. Temperatures shown: $\theta = 1.2$ (red), $\theta = 1.0$ (dark green), and $\theta = 0.7$ (blue).

free energy $f(m, h, \theta)$ then lies at $m > 0$ for any θ. At low temperatures, the double well structure we found in the $h = 0$ case is tilted so that the right well lies lower in energy than the left well. This is depicted in fig. 15.15. As the temperature is raised, the local minimum at $m < 0$ vanishes, annihilating with the local maximum in a saddle-node bifurcation. To find where this happens, one sets $\frac{\partial f}{\partial m} = 0$ and $\frac{\partial^2 f}{\partial m^2} = 0$ simultaneously, resulting in

$$h^*(\theta) = \sqrt{1-\theta} - \frac{\theta}{2} \ln\left(\frac{1+\sqrt{1-\theta}}{1-\sqrt{1-\theta}}\right). \tag{15.46}$$

The solutions lie at $h = \pm h^*(\theta)$. For $\theta < \theta_c = 1$ and $h \in \big[-h^*(\theta)\,,\,+h^*(\theta)\big]$, there are three solutions to the mean field equation. Equivalently we could in principle invert the above expression to obtain $\theta^*(h)$. For $\theta > \theta^*(h)$, there is only a single global minimum in the free energy $f(m)$ and there is no local minimum. Note $\theta^*(h = 0) = 1$.

15.3.2 Magnetization dynamics

Dissipative processes drive physical systems to minimum energy states. We can crudely model the dissipative dynamics of a magnet by writing the phenomenological equation

$$\frac{dm}{dt} = -\Gamma \frac{\partial f}{\partial m}\,. \tag{15.47}$$

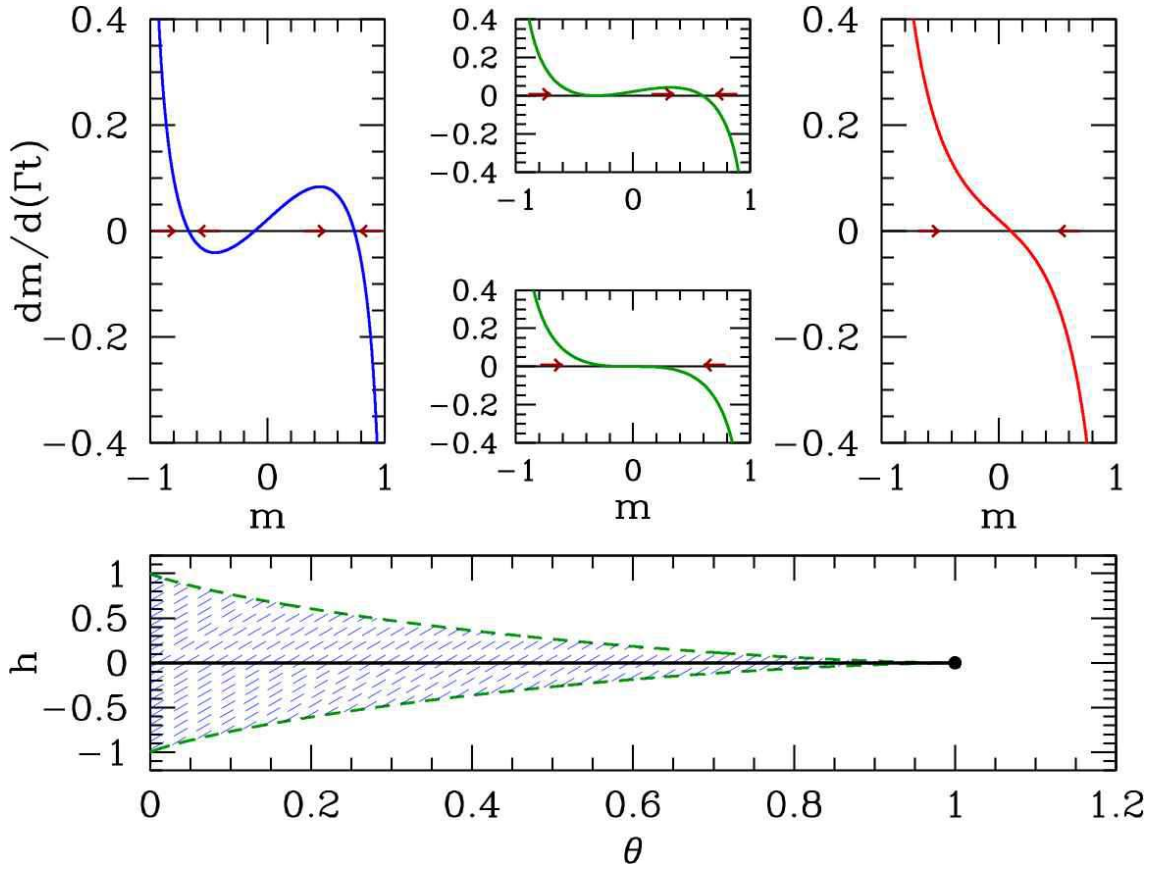

Figure 15.16: Dissipative magnetization dynamics $\dot{m} = -f'(m)$. Bottom panel shows $h^*(\theta)$ from eqn. 15.46. For (θ, h) within the blue shaded region, the free energy $f(m)$ has a global minimum plus a local minimum and a local maximum. Otherwise $f(m)$ has only a single global maximum. Top panels show an imperfect bifurcation in the magnetization dynamics at $h = 0.0215$, for which $\theta^* = 0.90$ Temperatures shown: $\theta = 0.80$ (blue), $\theta = \theta^*(h) = 0.90$ (green), and $\theta = 1.2$. The rightmost stable fixed point corresponds to the global minimum of the free energy. The bottom of the middle two upper panels shows $h = 0$, where both of the attractive fixed points and the repulsive fixed point coalesce into a single attractive fixed point (supercritical pitchfork bifurcation).

This drives the free energy f to smaller and smaller values:

$$\frac{df}{dt} = \frac{\partial f}{\partial m}\frac{dm}{dt} = -\Gamma\left(\frac{\partial f}{\partial m}\right)^2 \leq 0\,. \tag{15.48}$$

Clearly the *fixed point* of these dynamics, where $\dot{m} = 0$, is a solution to the mean field equation $\frac{\partial f}{\partial m} = 0$. At the solution to the mean field equation, one has

$$\frac{\partial f}{\partial m} = 0 \qquad \Rightarrow \qquad m = \tanh\left(\frac{m+h}{\theta}\right)\,. \tag{15.49}$$

The phase flow for the equation $\dot{m} = -\Gamma f'(m)$ is shown in fig. 15.16. As we have seen, for any value of h there is a temperature θ^* below which the free energy $f(m)$ has two local minima and one local

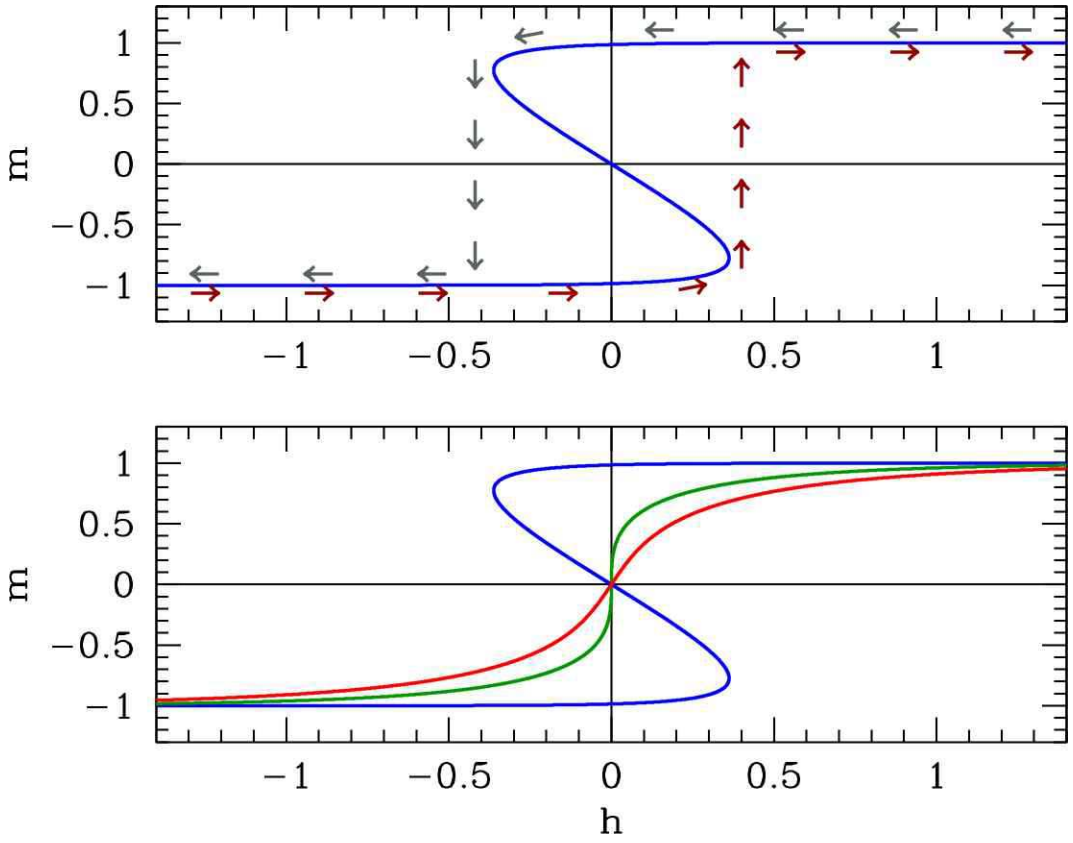

Figure 15.17: Top panel : hysteresis as a function of ramping the dimensionless magnetic field h at $\theta = 0.40$. Dark red arrows below the curve follow evolution of the magnetization on slow increase of h. Dark grey arrows above the curve follow evolution of the magnetization on slow decrease of h. Bottom panel : solution set for $m(\theta, h)$ as a function of h at temperatures $\theta = 0.40$ (blue), $\theta = \theta_{\rm c} = 1.0$ (dark green), and $t = 1.25$ (red).

maximum. When $h = 0$ the minima are degenerate, but at finite h one of the minima is a global minimum. Thus, for $\theta < \theta^*(h)$ there are three solutions to the mean field equations. In the language of dynamical systems, under the dynamics of eqn. 15.47, minima of $f(m)$ correspond to attractive fixed points and maxima to repulsive fixed points. If $h > 0$, the rightmost of these fixed points corresponds to the global minimum of the free energy. As θ is increased, this fixed point evolves smoothly. At $\theta = \theta^*$, the (metastable) local minimum and the local maximum coalesce and annihilate in a saddle-note bifurcation. However at $h = 0$ all three fixed points coalesce at $\theta = \theta_{\rm c}$ and the bifurcation is a supercritical pitchfork. As a function of t at finite h, the dynamics are said to exhibit an *imperfect bifurcation*, which is a deformed supercritical pitchfork.

The solution set for the mean field equation is simply expressed by inverting the $\tanh$ function to obtain $h(\theta, m)$. One readily finds

$$h(\theta, m) = \frac{\theta}{2} \ln\left(\frac{1+m}{1-m}\right) - m \ . \tag{15.50}$$

As we see in the bottom panel of fig. 15.17, $m(h)$ becomes multivalued for field values $h \in \big[-$

$h^*(\theta)\,,\,+h^*(\theta)\big]$, where $h^*(\theta)$ is given in eqn. 15.46. Now imagine that $\theta < \theta_{\rm c}$ and we slowly ramp the field h from a large negative value to a large positive value, and then slowly back down to its original value. On the time scale of the magnetization dynamics, we can regard $h(t)$ as a constant. Thus, $m(t)$ will flow to the nearest stable fixed point. Initially the system starts with $m = -1$ and h large and negative, and there is only one fixed point, at $m^* \approx -1$. As h slowly increases, the fixed point value m^* also slowly increases. As h exceeds $-h^*(\theta)$, a saddle-node bifurcation occurs, and two new fixed points are created at positive m, one stable and one unstable. The global minimum of the free energy still lies at the fixed point with $m^* < 0$. However, when h crosses $h = 0$, the global minimum of the free energy lies at the most positive fixed point m^*. The dynamics, however, keep the system stuck in what is a metastable phase. This persists until $h = +h^*(\theta)$, at which point another saddle-note bifurcation occurs, and the attractive fixed point at $m^* < 0$ annihilates with the repulsive fixed point. The dynamics then act quickly to drive m to the only remaining fixed point. This process is depicted in the top panel of fig. 15.17. As one can see from the figure, the the system follows a stable fixed point until the fixed point disappears, even though that fixed point may not always correspond to a global minimum of the free energy. The resulting $m(h)$ curve is then not reversible as a function of time, and it possesses a characteristic shape known as a *hysteresis loop*. Etymologically, the word *hysteresis* derives from the Greek $\upsilon\sigma\tau\varepsilon\rho\eta\sigma\iota\varsigma$, which means 'lagging behind'. Systems which are hysteretic exhibit a *history-dependence* to their status, which is not uniquely determined by external conditions. Hysteresis may be exhibited with respect to changes in applied magnetic field, changes in temperature, or changes in other externally determined parameters.

15.3.3 Cubic terms in Landau theory : first order transitions

Next, consider a free energy with a cubic term,

$$f = f_0 + \tfrac{1}{2}am^2 - \tfrac{1}{3}ym^3 + \tfrac{1}{4}bm^4\,, \tag{15.51}$$

with $b > 0$ for stability. Without loss of generality, we may assume $y > 0$ (else send $m \to -m$). Note that we no longer have $m \to -m$ (*i.e.* $\mathbb{Z}_2$) symmetry. The cubic term favors positive m. What is the phase diagram in the (a, y) plane?

Extremizing the free energy with respect to m, we obtain

$$\frac{\partial f}{\partial m} = 0 = am - ym^2 + bm^3\,. \tag{15.52}$$

This cubic equation factorizes into a linear and quadratic piece, and hence may be solved simply. The three solutions are $m = 0$ and

$$m = m_\pm \equiv \frac{y}{2b} \pm \sqrt{\left(\frac{y}{2b}\right)^2 - \frac{a}{b}}\,. \tag{15.53}$$

We now see that for $y^2 < 4ab$ there is only one real solution, at $m = 0$, while for $y^2 > 4ab$ there are three real solutions. Which solution has lowest free energy? To find out, we compare the energy $f(0)$ with $f(m_+)$[3]. Thus, we set

$$f(m) = f(0) \quad \Longrightarrow \quad \tfrac{1}{2}am^2 - \tfrac{1}{3}ym^3 + \tfrac{1}{4}bm^4 = 0\,, \tag{15.54}$$

[3]We needn't waste our time considering the $m = m_-$ solution, since the cubic term prefers positive m.

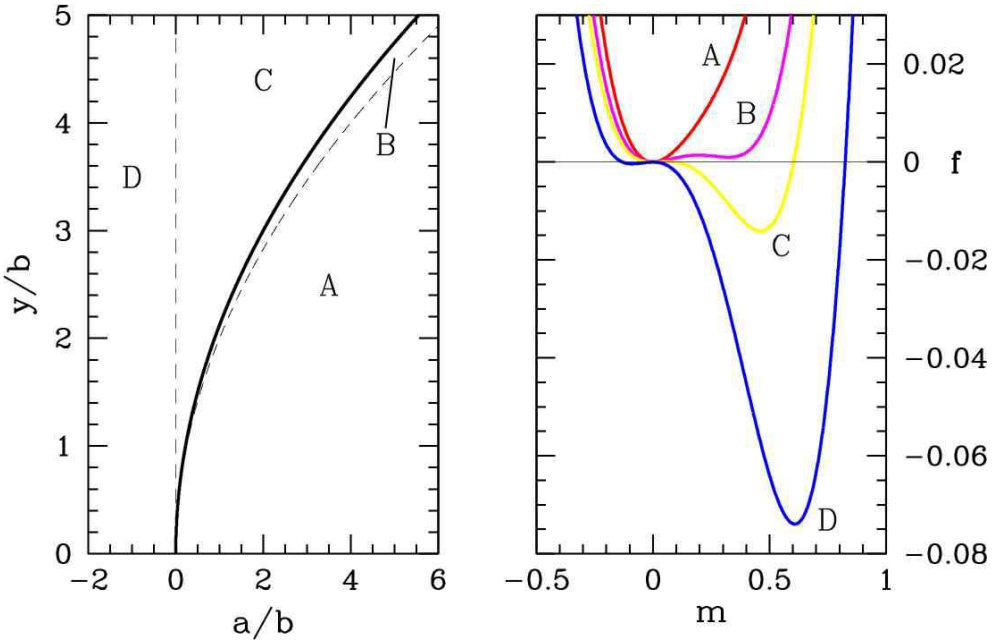

Figure 15.18: Behavior of the quartic free energy $f(m) = \frac{1}{2}am^2 - \frac{1}{3}ym^3 + \frac{1}{4}bm^4$. A: $y^2 < 4ab$; B: $4ab < y^2 < \frac{9}{2}ab$; C and D: $y^2 > \frac{9}{2}ab$. The thick black line denotes a line of first order transitions, where the order parameter is discontinuous across the transition.

and we now have two quadratic equations to solve simultaneously:

$$\begin{aligned} 0 &= a - ym + bm^2 \\ 0 &= \tfrac{1}{2}a - \tfrac{1}{3}ym + \tfrac{1}{4}bm^2 = 0 \, . \end{aligned} \tag{15.55}$$

Eliminating the quadratic term gives $m = 3a/y$. Finally, substituting $m = m_+$ gives us a relation between a, b, and y:

$$y^2 = \tfrac{9}{2}\, ab \, . \tag{15.56}$$

Thus, we have the following:

$$\begin{aligned} a > \frac{y^2}{4b} \quad &: \quad \text{1 real root } m = 0 \\ \frac{y^2}{4b} > a > \frac{2y^2}{9b} \quad &: \quad \text{3 real roots; minimum at } m = 0 \\ \frac{2y^2}{9b} > a \quad &: \quad \text{3 real roots; minimum at } m = \frac{y}{2b} + \sqrt{\left(\frac{y}{2b}\right)^2 - \frac{a}{b}} \end{aligned}$$

The solution $m = 0$ lies at a local minimum of the free energy for $a > 0$ and at a local maximum for $a < 0$. Over the range $\frac{y^2}{4b} > a > \frac{2y^2}{9b}$, then, there is a global minimum at $m = 0$, a local minimum at $m = m_+$, and a local maximum at $m = m_-$, with $m_+ > m_- > 0$. For $\frac{2y^2}{9b} > a > 0$, there is a local minimum at $a = 0$, a global minimum at $m = m_+$, and a local maximum at $m = m_-$, again with $m_+ > m_- > 0$. For $a < 0$, there is a local maximum at $m = 0$, a local minimum at $m = m_-$, and a global minimum at $m = m_+$, with $m_+ > 0 > m_-$. See fig. 15.18.

15.3.4 Magnetization dynamics

Suppose we now impose some dynamics on the system, of the simple relaxational type

$$\frac{dm}{dt} = -\Gamma \, \frac{\partial f}{\partial m} \, , \tag{15.57}$$

where Γ is a phenomenological kinetic coefficient. Assuming $y > 0$ and $b > 0$, it is convenient to adimensionalize by writing

$$m \equiv \frac{y}{b} \cdot u \qquad , \qquad a \equiv \frac{y^2}{b} \cdot \bar{r} \qquad , \qquad t \equiv \frac{b}{\Gamma y^2} \cdot s \, . \tag{15.58}$$

Then we obtain

$$\frac{\partial u}{\partial s} = -\frac{\partial \varphi}{\partial u} \, , \tag{15.59}$$

where the dimensionless free energy function is

$$\varphi(u) = \tfrac{1}{2}\bar{r}u^2 - \tfrac{1}{3}u^3 + \tfrac{1}{4}u^4 \, . \tag{15.60}$$

We see that there is a single control parameter, $\bar{r}$. The fixed points of the dynamics are then the stationary points of $\varphi(u)$, where $\varphi'(u) = 0$, with

$$\varphi'(u) = u\,(\bar{r} - u + u^2) \, . \tag{15.61}$$

The solutions to $\varphi'(u) = 0$ are then given by

$$u^* = 0 \qquad , \qquad u^* = \tfrac{1}{2} \pm \sqrt{\tfrac{1}{4} - \bar{r}} \, . \tag{15.62}$$

For $r > \frac{1}{4}$ there is one fixed point at $u = 0$, which is attractive under the dynamics $\dot{u} = -\varphi'(u)$ since $\varphi''(0) = \bar{r}$. At $\bar{r} = \frac{1}{4}$ there occurs a saddle-node bifurcation and a pair of fixed points is generated, one stable and one unstable. As we see from fig. 15.14, the interior fixed point is always unstable and the two exterior fixed points are always stable. At $r = 0$ there is a transcritical bifurcation where two fixed points of opposite stability collide and bounce off one another (metaphorically speaking).

At the saddle-node bifurcation, $\bar{r} = \frac{1}{4}$ and $u = \frac{1}{2}$, and we find $\varphi(u = \frac{1}{2}; \bar{r} = \frac{1}{4}) = \frac{1}{192}$, which is positive. Thus, the thermodynamic state of the system remains at $u = 0$ until the value of $\varphi(u_+)$ crosses zero. This occurs when $\varphi(u) = 0$ and $\varphi'(u) = 0$, the simultaneous solution of which yields $\bar{r} = \frac{2}{9}$ and $u = \frac{2}{3}$.

Suppose we slowly ramp the control parameter $\bar{r}$ up and down as a function of the dimensionless time s. Under the dynamics of eqn. 15.59, $u(s)$ flows to the first stable fixed point encountered – this is always the case for a dynamical system with a one-dimensional phase space. Then as $\bar{r}$ is further varied, u follows the position of whatever locally stable fixed point it initially encountered. Thus, $u\big(\bar{r}(s)\big)$ evolves smoothly until a bifurcation is encountered. The situation is depicted by the arrows in fig. 15.19. The equilibrium thermodynamic value for $u(\bar{r})$ is discontinuous; there is a first order phase transition at $\bar{r} = \frac{2}{9}$, as we've already seen. As r is increased, $u(\bar{r})$ follows a trajectory indicated by the magenta arrows. For an negative initial value of u, the evolution as a function of $\bar{r}$ will be *reversible*. However, if $u(0)$ is initially positive, then the system exhibits *hysteresis*, as shown. Starting with a large positive

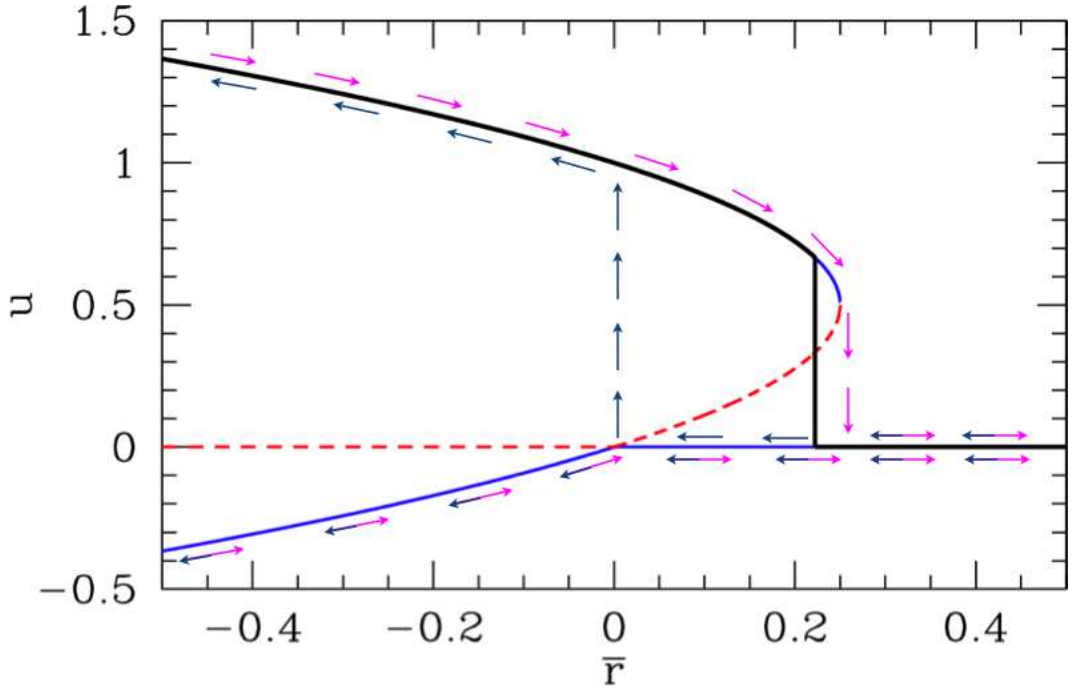

Figure 15.19: Fixed points for $\varphi(u) = \frac{1}{2}\bar{r}u^2 - \frac{1}{3}u^3 + \frac{1}{4}u^4$ and flow under the dynamics $\dot{u} = -\varphi'(u)$. Solid curves represent stable fixed points and dashed curves unstable fixed points. Magenta arrows show behavior under slowly increasing control parameter $\bar{r}$ and dark blue arrows show behavior under slowly decreasing $\bar{r}$. For $u > 0$ there is a hysteresis loop. The thick black curve shows the equilibrium thermodynamic value of $u(\bar{r})$, *i.e.* that value which minimizes the free energy $\varphi(u)$. There is a first order phase transition at $\bar{r} = \frac{2}{9}$, where the thermodynamic value of u jumps from $u = 0$ to $u = \frac{2}{3}$.

value of $\bar{r}$, $u(s)$ quickly evolves to $u = 0^+$, which means a positive infinitesimal value. Then as r is decreased, the system remains at $u = 0^+$ even through the first order transition, because $u = 0$ is an attractive fixed point. However, once r begins to go negative, the $u = 0$ fixed point becomes repulsive, and $u(s)$ quickly flows to the stable fixed point $u_+ = \frac{1}{2} + \sqrt{\frac{1}{4} - \bar{r}}$. Further decreasing r, the system remains on this branch. If $\bar{r}$ is later increased, then $u(s)$ remains on the upper branch past $r = 0$, until the u_+ fixed point annihilates with the unstable fixed point at $u_- = \frac{1}{2} - \sqrt{\frac{1}{4} - \bar{r}}$, at which time $u(s)$ quickly flows down to $u = 0^+$ again.

15.3.5 Sixth order Landau theory : tricritical point

Finally, consider a model with $\mathbb{Z}_2$ symmetry, with the Landau free energy

$$f = f_0 + \tfrac{1}{2}am^2 + \tfrac{1}{4}bm^4 + \tfrac{1}{6}cm^6 \,, \tag{15.63}$$

with $c > 0$ for stability. We seek the phase diagram in the (a, b) plane. Extremizing f with respect to m, we obtain

$$\frac{\partial f}{\partial m} = 0 = m\left(a + bm^2 + cm^4\right) , \tag{15.64}$$

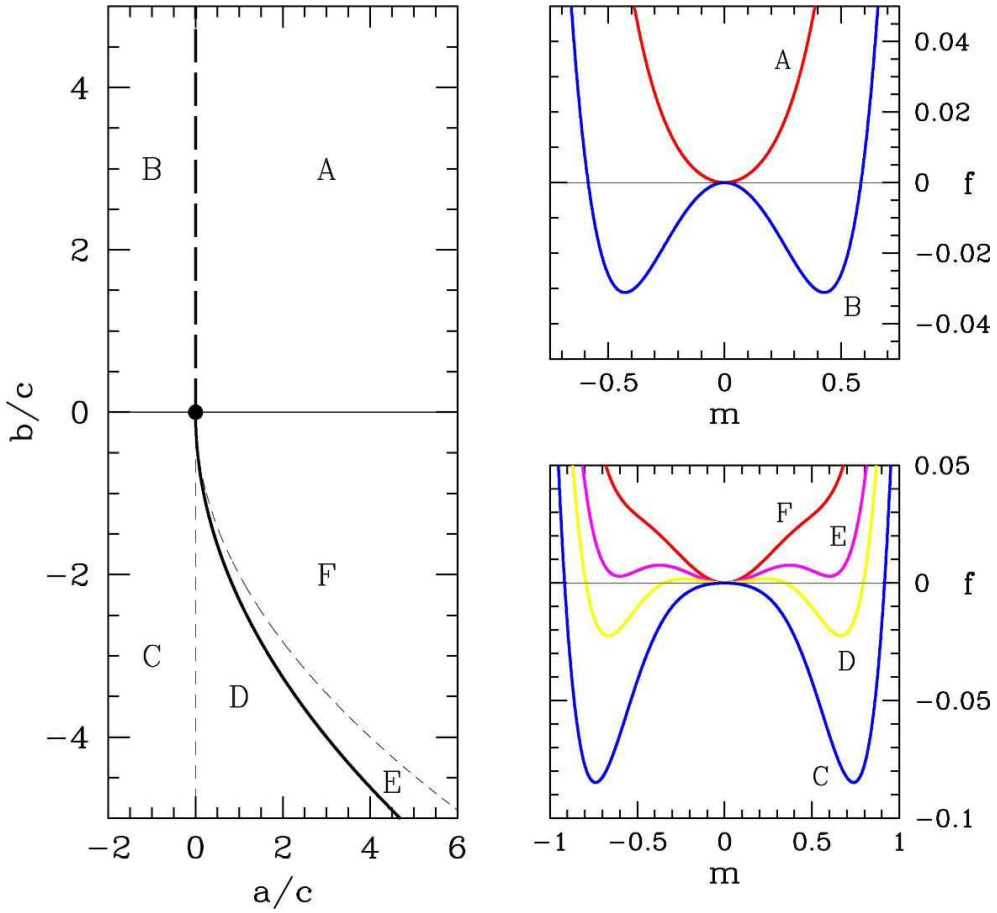

Figure 15.20: Behavior of the sextic free energy $f(m) = \frac{1}{2}am^2 + \frac{1}{4}bm^4 + \frac{1}{6}cm^6$. A: $a > 0$ and $b > 0$; B: $a < 0$ and $b > 0$; C: $a < 0$ and $b < 0$; D: $a > 0$ and $b < -\frac{4}{\sqrt{3}}\sqrt{ac}$; E: $a > 0$ and $-\frac{4}{\sqrt{3}}\sqrt{ac} < b < -2\sqrt{ac}$; F: $a > 0$ and $-2\sqrt{ac} < b < 0$. The thick dashed line is a line of second order transitions, which meets the thick solid line of first order transitions at the tricritical point, $(a, b) = (0, 0)$.

which is a quintic with five solutions over the complex m plane. One solution is obviously $m = 0$. The other four are

$$m = \pm\sqrt{-\frac{b}{2c} \pm \sqrt{\left(\frac{b}{2c}\right)^2 - \frac{a}{c}}}\,. \tag{15.65}$$

For each $\pm$ symbol in the above equation, there are two options, hence four roots in all.

If $a > 0$ and $b > 0$, then four of the roots are imaginary and there is a unique minimum at $m = 0$.

For $a < 0$, there are only three solutions to $f'(m) = 0$ for real m, since the $-$ choice for the $\pm$ sign under the radical leads to imaginary roots. One of the solutions is $m = 0$. The other two are

$$m = \pm\sqrt{-\frac{b}{2c} + \sqrt{\left(\frac{b}{2c}\right)^2 - \frac{a}{c}}}\,. \tag{15.66}$$

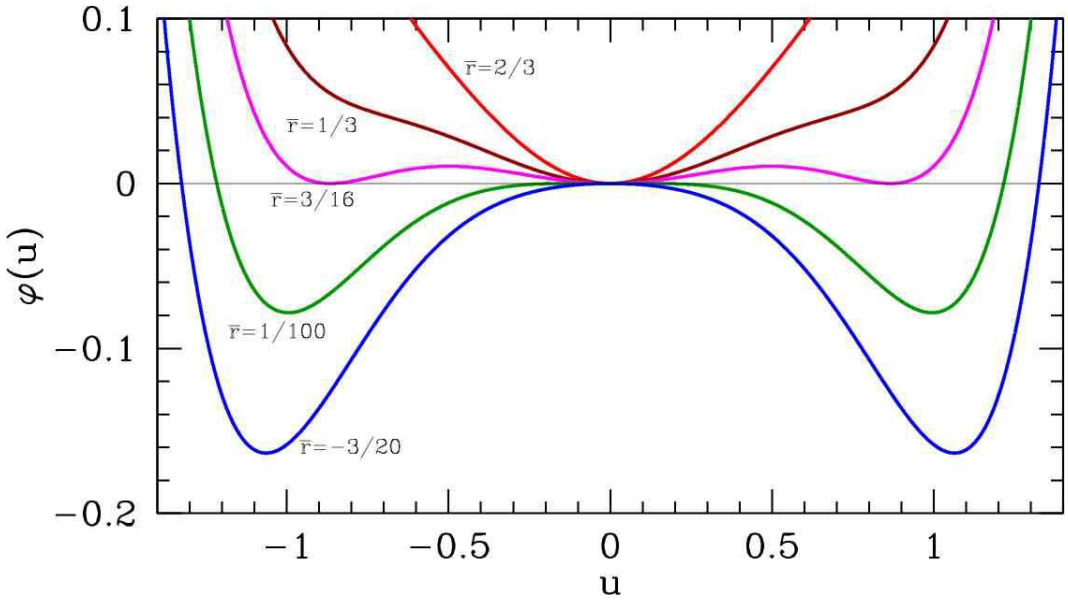

Figure 15.21: Free energy $\varphi(u) = \frac{1}{2}\bar{r}u^2 - \frac{1}{4}u^4 + \frac{1}{6}u^6$ for several different values of the control parameter $\bar{r}$.

The most interesting situation is $a > 0$ and $b < 0$. If $a > 0$ and $b < -2\sqrt{ac}$, all five roots are real. There must be three minima, separated by two local maxima. Clearly if m^* is a solution, then so is $-m^*$. Thus, the only question is whether the outer minima are of lower energy than the minimum at $m = 0$. We assess this by demanding $f(m^*) = f(0)$, where m^* is the position of the largest root (*i.e.* the rightmost minimum). This gives a second quadratic equation,

$$0 = \tfrac{1}{2}a + \tfrac{1}{4}bm^2 + \tfrac{1}{6}cm^4 \,, \tag{15.67}$$

which together with equation 15.64 gives

$$b = -\tfrac{4}{\sqrt{3}}\sqrt{ac}\,. \tag{15.68}$$

Thus, we have the following, for fixed $a > 0$:

$$\begin{aligned} b > -2\sqrt{ac} \quad &: \quad \text{1 real root } m = 0 \\ -2\sqrt{ac} > b > -\tfrac{4}{\sqrt{3}}\sqrt{ac} \quad &: \quad \text{5 real roots; minimum at } m = 0 \\ -\tfrac{4}{\sqrt{3}}\sqrt{ac} > b \quad &: \quad \text{5 real roots; minima at } m = \pm\sqrt{-\frac{b}{2c} + \sqrt{\Big(\frac{b}{2c}\Big)^2 - \frac{a}{c}}} \end{aligned}$$

The point $(a, b) = (0, 0)$, which lies at the confluence of a first order line and a second order line, is known as a *tricritical point*.

15.3.6 Hysteresis for the sextic potential

Once again, we consider the dissipative dynamics $\dot{m} = -\Gamma\, f'(m)$. We adimensionalize by writing

$$m \equiv \sqrt{\frac{|b|}{c}} \cdot u \qquad , \qquad a \equiv \frac{b^2}{c} \cdot \bar{r} \qquad , \qquad t \equiv \frac{c}{\Gamma\, b^2} \cdot s \; . \tag{15.69}$$

Then we obtain once again the dimensionless equation

$$\frac{\partial u}{\partial s} = -\frac{\partial \varphi}{\partial u} \; , \tag{15.70}$$

where

$$\varphi(u) = \tfrac{1}{2}\bar{r}u^2 \pm \tfrac{1}{4}u^4 + \tfrac{1}{6}u^6 \; . \tag{15.71}$$

In the above equation, the coefficient of the quartic term is positive if $b > 0$ and negative if $b < 0$. That is, the coefficient is $\mathrm{sgn}(b)$. When $b > 0$ we can ignore the sextic term for sufficiently small u, and we recover the quartic free energy studied earlier. There is then a second order transition at $r = 0$. .

New and interesting behavior occurs for $b > 0$. The fixed points of the dynamics are obtained by setting $\varphi'(u) = 0$. We have

$$\begin{aligned} \varphi(u) &= \tfrac{1}{2}\bar{r}u^2 - \tfrac{1}{4}u^4 + \tfrac{1}{6}u^6 \\ \varphi'(u) &= u\,(\bar{r} - u^2 + u^4) \; . \end{aligned} \tag{15.72}$$

Thus, the equation $\varphi'(u) = 0$ factorizes into a linear factor u and a quartic factor $u^4 - u^2 + \bar{r}$ which is quadratic in u^2. Thus, we can easily obtain the roots:

$$\begin{aligned} \bar{r} < 0 \quad &: \quad u^* = 0 \; , \; u^* = \pm\sqrt{\tfrac{1}{2} + \sqrt{\tfrac{1}{4} - \bar{r}}} \\ 0 < \bar{r} < \tfrac{1}{4} \quad &: \quad u^* = 0 \; , \; u^* = \pm\sqrt{\tfrac{1}{2} + \sqrt{\tfrac{1}{4} - \bar{r}}} \; , \; u^* = \pm\sqrt{\tfrac{1}{2} - \sqrt{\tfrac{1}{4} - \bar{r}}} \\ \bar{r} > \tfrac{1}{4} \quad &: \quad u^* = 0 \; . \end{aligned} \tag{15.73}$$

In fig. 15.22, we plot the fixed points and the hysteresis loops for this system. At $\bar{r} = \frac{1}{4}$, there are two symmetrically located saddle-node bifurcations at $u = \pm\frac{1}{\sqrt{2}}$. We find $\varphi(u = \pm\frac{1}{\sqrt{2}}, \bar{r} = \frac{1}{4}) = \frac{1}{48}$, which is positive, indicating that the stable fixed point $u^* = 0$ remains the thermodynamic minimum for the free energy $\varphi(u)$ as $\bar{r}$ is decreased through $\bar{r} = \frac{1}{4}$. Setting $\varphi(u) = 0$ and $\varphi'(u) = 0$ simultaneously, we obtain $\bar{r} = \frac{3}{16}$ and $u = \pm\frac{\sqrt{3}}{2}$. The thermodynamic value for u therefore jumps discontinuously from $u = 0$ to $u = \pm\frac{\sqrt{3}}{2}$ (either branch) at $\bar{r} = \frac{3}{16}$; this is a first order transition.

Under the dissipative dynamics considered here, the system exhibits hysteresis, as indicated in the figure, where the arrows show the evolution of $u(s)$ for very slowly varying $\bar{r}(s)$. When the control parameter $\bar{r}$ is large and positive, the flow is toward the sole fixed point at $u^* = 0$. At $\bar{r} = \frac{1}{4}$, two simultaneous saddle-node bifurcations take place at $u^* = \pm\frac{1}{\sqrt{2}}$; the outer branch is stable and the inner branch unstable in both cases. At $r = 0$ there is a subcritical pitchfork bifurcation, and the fixed point at $u^* = 0$ becomes unstable.

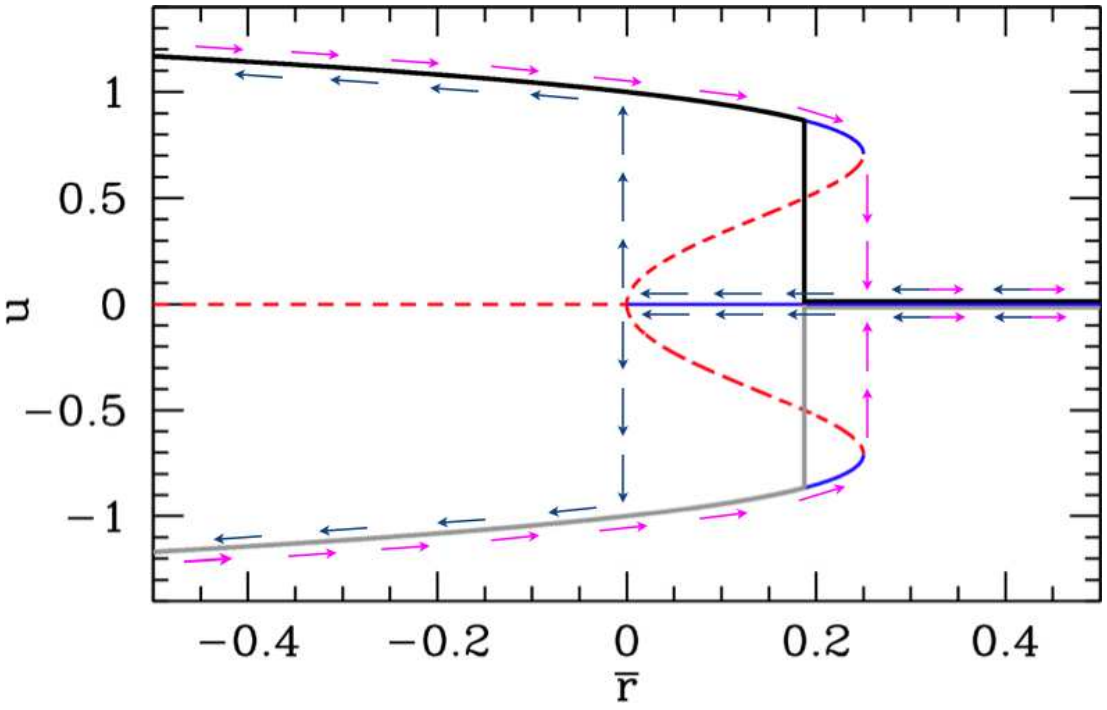

Figure 15.22: Fixed points $\varphi'(u^*) = 0$ for the sextic potential $\varphi(u) = \frac{1}{2}\bar{r}u^2 - \frac{1}{4}u^4 + \frac{1}{6}u^6$, and corresponding dynamical flow (arrows) under $\dot{u} = -\varphi'(u)$. Solid curves show stable fixed points and dashed curves show unstable fixed points. The thick solid black and solid grey curves indicate the equilibrium thermodynamic values for u; note the overall $u \to -u$ symmetry. Within the region $\bar{r} \in [0, \frac{1}{4}]$ the dynamics are irreversible and the system exhibits the phenomenon of hysteresis. There is a first order phase transition at $\bar{r} = \frac{3}{16}$.

Suppose one starts off with $\bar{r} \gg \frac{1}{4}$ with some value $u > 0$. The flow $\dot{u} = -\varphi'(u)$ then rapidly results in $u \to 0^+$. This is the 'high temperature phase' in which there is no magnetization. Now let r increase slowly, using s as the dimensionless time variable. The scaled magnetization $u(s) = u^*\big(\bar{r}(s)\big)$ will remain pinned at the fixed point $u^* = 0^+$. As $\bar{r}$ passes through $\bar{r} = \frac{1}{4}$, two new stable values of u^* appear, but our system remains at $u = 0^+$, since $u^* = 0$ is a stable fixed point. But after the subcritical pitchfork, $u^* = 0$ becomes unstable. The magnetization $u(s)$ then flows rapidly to the stable fixed point at $u^* = \frac{1}{\sqrt{2}}$, and follows the curve $u^*(\bar{r}) = \big(\frac{1}{2} + (\frac{1}{4} - \bar{r})^{1/2}\big)^{1/2}$ for all $r < 0$.

Now suppose we start increasing r (*i.e.* increasing temperature). The magnetization follows the stable fixed point $u^*(\bar{r}) = \big(\frac{1}{2} + (\frac{1}{4} - \bar{r})^{1/2}\big)^{1/2}$ past $\bar{r} = 0$, beyond the first order phase transition point at $\bar{r} = \frac{3}{16}$, and all the way up to $\bar{r} = \frac{1}{4}$, at which point this fixed point is annihilated at a saddle-node bifurcation. The flow then rapidly takes $u \to u^* = 0^+$, where it remains as r continues to be increased further.

Within the region $\bar{r} \in \big[0, \frac{1}{4}\big]$ of control parameter space, the dynamics are said to be *irreversible* and the behavior of $u(s)$ is said to be *hysteretic*.